



Dorado Build 1 Fore and Sternplane Redesign

George D. Watt

Defence R&D Canada

Technical Memorandum

DRDC Atlantic TM 2002-048

September 2002

This page intentionally left blank.

Dorado Build 1 Fore and Sternplane Redesign

George D. Watt

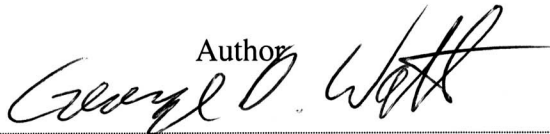
Defence R&D Canada – Atlantic

Technical Memorandum

DRDC Atlantic TM 2002-048

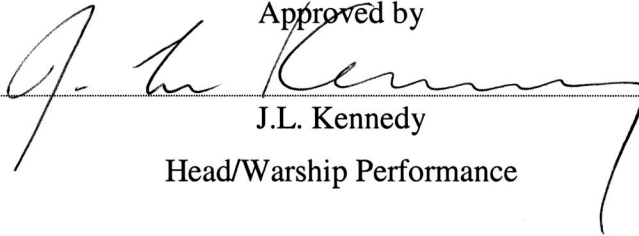
September 2002

Author



George D. Watt

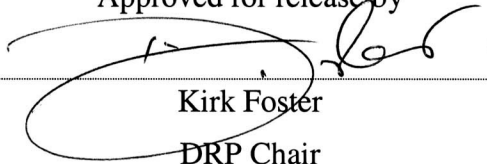
Approved by



J.L. Kennedy

Head/Warship Performance

Approved for release by



Kirk Foster

DRP Chair

The body of this document was prepared using the Maple software package which integrates calculations and text in a single environment. This leads to some deviations from the DRDC standard format.

Abstract

The Dorado semi-submersible remote minehunting vehicle requires increased pitch, roll, and depth control while towing its sonar at depth. The vehicle controls both pitch and roll using independently deflectable sternplanes. Depth is controlled with foreplanes. New fore and sternplane designs are proposed which double control authority with about a 20% increase in span length and a 60% increase in average chord length. The new designs require from 3 to 4 times more actuator torque to achieve control and the actuator shaft bending moment will be up to 4 times larger. However, the new plane designs should allow the vehicle to maintain depth and equilibrium with only moderate control deflections while towing the sonar at depth.

Résumé

Le véhicule télécommandé semi-submersible de chasse aux mines Dorado a besoin d'un meilleur contrôle du tangage, du roulis et de la profondeur lorsqu'il remorque son sonar en profondeur. Il contrôle le tangage et le roulis au moyen de volets arrière inclinables de façon indépendante. La profondeur est contrôlée par des volets avant. Les nouveaux modèles de volets proposés doublent le pouvoir de commande pour une augmentation d'environ 20% de l'envergure et de 60% de la longueur moyenne de la corde. Ces nouveaux modèles exigent un couple de vérin de 3 à 4 fois supérieur pour réaliser le contrôle et le moment de courbure de l'axe du vérin peut être multiplié par 4. Cependant, ils devraient permettre au véhicule de chasse aux mines de maintenir sa profondeur et son équilibre par des déflexions modérées des volets pendant le remorquage du sonar en profondeur.

This page intentionally left blank.

Executive summary

Introduction

DRDC Atlantic has developed, and is now supporting a Technical Demonstration of, a Remote Minehunting System (RMS). The RMS uses a remote drone (called Dorado) to tow a sonar at depths up to 200 m for minehunting purposes. Dorado maneuvers using its sternplanes for pitch and roll control and its foreplanes for depth control. In recent trials, these planes reached their limits without providing adequate control. The objective of this report is to document new fore and sternplane designs that substantially improve the control authority of these planes.

Principle Results

New designs are proposed which double control authority with only modest increases in the span length of the planes. Although, substantially larger actuator loads will be encountered with these new planes, using them should allow the vehicle to maintain depth and equilibrium while towing its sonar at maximum depth without aid from the ballast tanks.

Significance of Results

The new designs should allow improved Dorado maneuvering during minehunting tasks. They result in a more robust minehunting system.

Future Plans

Work is underway to try to implement these designs in time for the next set of Dorado sea trials, in order to evaluate the new designs.

Watt, G.D; 2002; Dorado Build 1 Fore and Sternplane Redesign; DRDC Atlantic TM 2002-048; Defence R&D Canada – Atlantic.

Sommaire

Introduction

DRDC Atlantique a mis au point et assure maintenant le support de démonstration technique d'un système télécommandé de chasse aux mines (RMS). Le RMS utilise un drone télécommandé (appelé Dorado) pour remorquer un sonar à une profondeur maximale de 200 m pour la chasse aux mines. Dorado utilise des volets arrière pour les commandes de tangage et de roulis et des volets avant pour contrôler la profondeur. Lors d'essais récents, ces volets ont atteint leurs limites sans fournir un contrôle adéquat. L'objet de ce rapport est de documenter de nouveaux modèles de volets avant et arrière qui améliorent de façon significative le pouvoir de contrôle.

Principaux résultats

Les nouveaux modèles proposés doublent le pouvoir de contrôle pour une légère augmentation de l'envergure des volets. Bien que les charges exercées sur les vérins soient nettement supérieures sur ces nouveaux modèles, le véhicule serait capable de maintenir sa profondeur et son équilibre pendant qu'il remorque son sonar à la profondeur maximale sans l'aide des citernes de ballast.

Importance des résultats

Les nouveaux modèles devraient permettre d'améliorer les manœuvres du Dorado durant les missions de chasse aux mines. La robustesse du système de chasse aux mines en sera améliorée.

Plans futurs

Des travaux sont en cours pour améliorer ces modèles à temps pour la prochaine série d'essais en mer du Dorado, afin d'évaluer les nouveaux modèles.

Watt, G.D; 2002; Dorado Build 1 Fore and Sternplane Redesign; DRDC Atlantic TM 2002-048; Defence R&D Canada – Atlantic.

Table of contents

Abstract.....	i
Résumé	i
Executive summary	iii
Sommaire.....	iv
Table of contents	v
List of figures	vii
List of symbols	viii
Introduction	1
Current Design (Build 1)	2
Sternplane Effectiveness and Pitch Control.....	4
Sternplane Cantilever Moment.....	6
Sternplane Roll Control	7
Foreplane Forces	10
New Sternplane Design.....	11
Magenta Design Characteristics	14
Magenta Design Loads	15
New Foreplane Design.....	16
Green Design Characteristics	20
Green Design Loads.....	20

Minimizing Actuator Torque Requirements	21
Appendage Drag During Deep Tow Conditions.....	22
Discussion	23
Concluding Remarks.....	24
References	25
Appendix A: Sternplane Magenta Design.....	26
Appendix B: Foreplane Green Design	29
Appendix C: Mold Geometry	31

List of figures

Figure 1. Dorado Build 1 Vertical Plane Control Geometry: Planform View.....	2
Figure 2. Pitch Control vs. Root Chord at Fixed Span (Red) or Tip Chord (Blue) Lengths; Sweepback = 20 Degrees	12
Figure 3. Roll Control vs. Root Chord at Fixed Span (Red) or Tip Chord (Blue) Lengths; Sweepback = 20 Degrees.....	12
Figure 4. The Build 1 (red) and Three Sweptback Designs and Their Design CP's (+).....	13
Figure 5. Dominant Deep Tow, Even Keel Forces.....	17
Figure 6. The Build 1 (red) and New (solid green) Foreplane and its Design CP (+).....	19
Figure 7. The L.E. Root (red) and Tip (blue) Section Profiles.....	27
Figure 8. Magenta Design - Starboard Sternplane.....	28
Figure 9. Magenta Design - Line Drawing	28
Figure 10. Green Design - Line Drawing.....	30
Figure 11. Dorado Fore and Sternplane Mold Planform (x,y) coordinates in Meters.....	31
Figure 12. Mold Half-Thickness Distribution (meters) Along Actuator Shaft Axes	32

List of Symbols

a	isolated wing (exposed wing area) effective aspect ratio $(b - d)^2/S_a$.
A	isolated wing (embedded in hull) effective aspect ratio b^2/S_A .
b	fore or sternplane tip-to-tip span length.
c	wing chord length (mean chord unless subscripted).
C_L, C_D	wing lift and drag coefficients, nondimensionalized with S .
d, D	local and maximum hull diameters.
D	drag.
K	rolling moment, nondimensionalized with $\rho U^2 l^3/2$.
$K_{W(B)},$ $K_{B(W)}$	ratios of lift on the wing (in the presence of the body) and lift on the body (in the presence of the wing) to the lift on an isolated wing based on <i>exposed</i> wing area S_a .
l	overall hull length.
L	lift.
M_c	cantilever moment; roll moment of a deflecting plane about its pedestal.
Q	dynamic pressure $\rho U^2/2$.
S	wing planform area.
t	airfoil section thickness.
T	tow cable tension.
u, w	forward and vertical body axis velocities.
U	overall velocity.
$W(\lambda, A)$	dimensionless rolling moment from an isolated wing with differentially deflecting tips.
$WBF(\lambda, A)$	dimensionless rolling moment from differentially deflecting horizontal wings on a body with fixed vertical fin.
x, y	nonstandard body fixed axes.
Z	body normal force, nondimensionalized with $\rho U^2 l^2/2$.
α	angle of attack: $\tan^{-1}(w/u)$
γ	angle tow cable makes with the horizontal.
δ_f, δ_s	fore and sternplane control surface deflection angles.
η	NACA airfoil half-thickness profile normalized by chord length: $\eta(\xi)$.
η_s	sternplane efficiency.
λ, Λ	local d and maximum D hull diameter to span ratios.
ξ	chordwise coordinate in NACA airfoil thickness distribution $\eta(\xi)$, normalized by chord length.
ρ	fluid density.
Ω	sweepback angle of wing quarter chord line.

Introduction

The Dorado semi-submersible remote minehunting vehicle requires increased roll, pitch, and depth control authority. The vehicle controls both pitch and roll by using independently deflectable, horizontal sternplanes. Depth is controlled by dedicated foreplanes.

The best way to increase pitch and roll control would be to take roll control away from the sternplanes and give it to an active flap on the snorkle fairing (where the leverage is greatest). And the best way to implement control surface depth control would be to move the foreplanes down to the keel thereby minimizing wake interference with the sternplanes. However, these would be major changes requiring new systems and control algorithms. So the solution pursued here is to retain all current control functionality and simply increase fore and sternplane size. This solution is intended for the Dorado Build 3 trials in the Fall of 2002.

We begin by estimating the control authority of the current planes. New designs are then proposed and evaluated using the same estimation procedures. The new sternplane design doubles the control authority with a 20% increase in span length and a 60% increase in average chord length. The new foreplane is sized to balance the new sternplane pitch control capability for deep tow conditions. It increases depth control by 90% using the same span length and planform end geometry as the new sternplane.

Unlike the current planes, the new designs are tapered in the spanwise direction with a leading edge sweepback of 20 degrees. This improves efficiency, allows for a large diameter actuator shaft at the root, and allows the section profile maximum thickness to be reduced from a bluff 25% to an optimum 15% of chord. The foreplane design is identical to the end of the sternplane design, which minimizes manufacturing costs.

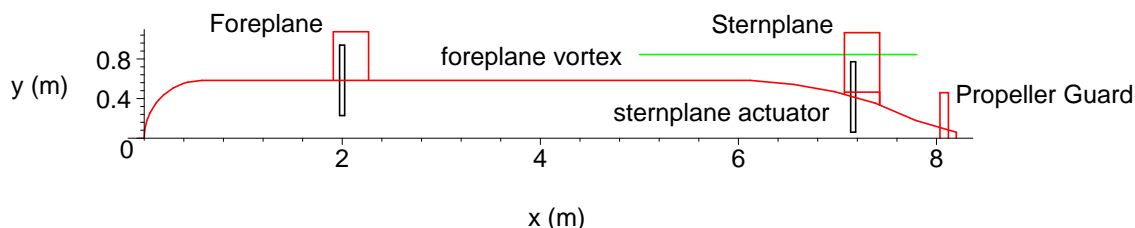
The actuator for the new planes will probably have to generate from 3 to 4 times more torque than for the current planes. And its shaft should be able to support from 3 to 4 times the cantilever (bending) moment at the root.

It is estimated that the new fore and sternplanes will be able to maintain vehicle depth with zero pitch under high load conditions with moderate deflections of about 5 and 10 degrees, respectively.

Current Design (Build 1)

The current design is shown in Figure 1. Note that the sternplanes deflect on pedestals.

Fig. 1: Dorado Build 1 Vertical Plane Control Geometry: Planform View



The foreplanes are used only for depth control. There is concern about interference of the foreplane trailing wake with the sternplanes. Spreiter and Sacks [1] show that the wake of a low aspect ratio wing rolls up into a discrete vortex within a few chord lengths. The spanwise location of the core of a rolled up vortex trailing from an elliptically loaded isolated wing is at $\pi/4$ of its semi-span. This ratio is used to estimate the location of the foreplane vortex at the sternplanes in the above figure. It is shown as a green line.

Downwash interactions of this type are notoriously volatile and difficult to predict. The foreplane vortex location may be above or below the sternplane, depending on the pitch history, and will be influenced by both the hull and the horizontal plane maneuvering history. Nevertheless, given that the fore and sternplanes are nominally in-line and of the same dimensions, it is probably good that the vortex is inboard of the sternplane tip as this tends to average out upwash and downwash effects from the vortex. The operators have not noticed adverse effects from the current configuration, which has the same tip-to-tip span for both the fore and sternplanes, so the new design will maintain this relationship. To improve control, however, the span and chord lengths of the planes will be increased, so any interactions that are now present will increase in magnitude relative to the inertia of the vehicle. Thus, these interactions may become noticeable.

The effect of sternplane downwash on the propeller will increase to the extent that the new sternplanes can achieve a higher lift to span squared ratio (L/b^2). The uniform deflections of pitch control generate strong tip vortices from the sternplanes that are well outboard of the propeller. Theoretically, with uniform deflection along the entire span, the tip vortices join each other across the span of the sternplanes and through the body, again well away from the propeller. The net effect of this U-shaped vortex system is a uniform downwash in the middle of the U, where the propeller is located, that is proportional to the L/b^2 ratio of the wing [1]. This ratio increases by about 1.4 with the new sternplane design.

The problem with this simplified scenario is that the wing does not deflect through the hull. Indeed, there is necessarily a gap between the sternplane and its pedestal which tends to equalize the pressure difference across the inboard end of the plane. In addition, the fixed pedestal, with its own kutta condition to satisfy, cannot sustain the circulation generated by the deflecting portion of the plane. As a result, it is expected that vorticity is also shed from the inboard end of the deflecting plane. This may in fact reduce the net downwash along the centerline of the propeller, but it makes for potentially large velocity variations immediately downstream of the sternplane root.

It is not clear whether using sternplanes for roll control aggravates this problem. It is theoretically necessary for circulation of opposite sense, from differentially deflected planes, to trail vorticity from inboard the deflecting planes. Conservation of circulation requires that this circulation must either be shed at the sternplane roots or bind with that from across the hull to create a doubly strong hull bound vortex trailing aft from the sternplanes along the hull centerline. A strong hull bound vortex co-axial with the propeller generates an axisymmetric effect that should not load the propeller unsteadily. But vorticity shed from the sternplane roots will load the propeller unsteadily.

The current propeller does suffer cavitation damage. If this cavitation is the result of vorticity shed from the sternplanes, then we can expect the problem to be aggravated to the extent that the downwash velocity field (L/b^2 ratio) is increased by the new design.

In the analyses below, a combination of theory and empiricism is used to estimate the lifts and rolling moment generated by the fore and sternplanes. These forces are easiest to calculate relative to the lift on an isolated wing. For example, Pitts *et al* [2] use slender body theory to show that the overall lift generated by the addition of a wing to a slender cylindrical body in a flow at incidence α is:

$$L_{\alpha} = (K_{W(B)} + K_{B(W)}) L_W$$

where L_W is the lift on the exposed half-wings joined together (with their tip-to-tip span $= b - d$, where b is the tip-to-tip span of the wing on the body and d is the body diameter), $K_{W(B)}$ is a dimensionless coefficient giving the lift on the wing in the presence of the body, and $K_{B(W)}$ gives the lift on the body in the presence of the wing. Slender body theory overpredicts L_W unless the wing aspect ratio is less than 1 (which is unusual). So a semi-empirical formula that takes better account of aspect ratio is commonly used to estimate L_W . Herein, we estimate the lift curve slope on an isolated wing using the formula developed by Whicker and Fehlner [3]:

$$\frac{\partial}{\partial \alpha} C_L = 1.8 \frac{\pi A}{1.8 + \cos(\Omega) \sqrt{\frac{A^2}{\cos(\Omega)^4} + 4}}$$

where A is the effective aspect ratio, Ω is the sweepback angle of the quarter chord line, C_L is the lift coefficient of the wing nondimensionalized by S , and S is the wing planform area.

The slender body theory prediction for $K_{W(B)} + K_{B(W)}$ is good for planes attached to a parallel body with no appreciable boundary layer, such as the foreplanes. In other words, slender body theory does a good job of predicting the relative change in L_w that accounts for lift carry over to the hull and interference of the hull with the planes, even though it doesn't necessarily predict L_w itself satisfactorily. This philosophy, of using semi-empirical methods where they are required and slender body theory to account for relative change due to some geometrical perturbation, is also used for predicting pitch, roll, and depth control derivatives.

The sternplane analysis is carried out first. Because sternplanes are attached to a contracting afterbody in the presence of a large boundary layer, the slender body theory $K_{W(B)} + K_{B(W)}$ interference estimate is inadequate for predicting incidence lift. A semi-empirical method must be used. A confusing complication of this method is that it is based on the lift on an isolated wing with the actual tip-to-tip span of the sternplanes and a surface area obtained by removing the hull and extending the current leading and trailing edges in straight lines until they meet at the centerline.

So, in what follows, L_w will always refer to the smaller isolated wing formed by joining together the exposed half-wings. Its aspect ratio is $a = (b - d)^2 / S_a = (b - d) / c_a$ where $S_a = (b - d) c_a$ is the wing planform area and c_a is the mean chord length. The large isolated wing will be identified by the use of $A = b^2 / S_A = b / c_A$ for aspect ratio, where $S_A = b c_A$ is the wing area and c_A is the mean chord length. Note that c_A is larger than c_a if the planform is tapered since this taper extends to the centerline.

Sternplane Effectiveness and Pitch Control

Dempsey [4] shows that sternplane normal force can be estimated semi-empirically by multiplying the lift curve slope of an isolated wing (based on full sternplane span) by a *sternplane efficiency*, a semi-empirical expression that accounts for the loss of lift resulting from the wing being embedded in both the hull and the hull boundary layer. Sternplane efficiency η_s is always less than one:

$$\eta_s = 1 - .2556 \Lambda \sqrt{1 - .1612 \Lambda^2} - .6366 \arcsin(.4015 \Lambda)$$

for

$$0 < \Lambda < 2.5$$

where $\Lambda = D/b$ is the inverse span parameter and D is the maximum hull diameter. Using the Whicker and Fehlner formula for lift curve slope, Dempsey gives the sternplane contribution to the normal force derivative Z_w as:

$$\Delta Z_w = -1.8 \frac{\pi b^2 (1 - .2556 \Lambda \sqrt{1 - .1612 \Lambda^2 - .6366 \arcsin(.4015 \Lambda)})}{\left(1.8 + \cos(\Omega) \sqrt{\frac{A^2}{\cos(\Omega)^4} + 4}\right) l^2}$$

Since C_L is nondimensionalized by $S_A = b^2/A$ and ΔZ_w is nondimensionalized by l^2 (the convention in submarine hydrodynamics), a conversion is made in the above formula. ΔZ_w gives the sternplane effectiveness which contributes to the vertical plane stability of the vehicle.

Pitch control is determined by how much Z changes when the sternplanes are synchronously deflected an angle δ_s on their pedestals and is given by:

$$\frac{\partial}{\partial \delta_s} Z = Z_{\delta_s}$$

Slender body theory is used to estimate the relative magnitude of lift from a pitch control deflection δ relative to lift from incidence α for a wing body combination. Pitts *et al* [2] quote the result for overall lift due to deflection δ and this can be simplified to:

$$L_\delta = K_{W(B)} L_w$$

so that:

$$\frac{L_\delta}{L_\alpha} = \frac{1}{1 + \frac{K_{B(W)}}{K_{W(B)}}}$$

Slender body theory derived analytical expressions for $K_{W(B)}$ and $K_{B(W)}$ are provided by Pitts *et al* but it is approximately true that $K_{B(W)}/K_{W(B)} = d/b$, where d is the local hull diameter. Since Dorado's contracting afterbody is not cylindrical and slender body theory does not account for the boundary layer present at the sternplane, the d value to use here is not clearly defined. However recent experiments, still undergoing analysis, suggest the hull diameter at the leading edge root is a good choice. This is consistent with a slender body view of the flow where lift is generated at the leading edge. Thus:

$$Z_{\delta_s} = \frac{\Delta Z_w}{1 + \lambda}$$

where $\lambda = d/b$. In other words, while we account for the boundary layer in the calculation of ΔZ_w , we assume the boundary layer does not play a major roll in the $Z_{\delta_s}/\Delta Z_w$ ratio.

As the appendage span goes to infinity (λ goes to zero), there is no difference between a δ

deflection and overall incidence; the hull is inconsequential. However, as the span becomes increasingly small (b approaches d , λ goes to 1), uniformly deflecting sternplanes generate only half the total lift they generate when the hull deflects with them.

The current Dorado sternplane dimensions (in meters) have been estimated from a scale drawing as:

leading edge root coordinates $(x,y) = (7.070, .442)$

chord $= .356$

tip-to-tip span $b = 2.132$

hull length $l = 8.2$

maximum hull diameter $D = 1.168$

$\Lambda, \lambda = .5480, .4146$

effective aspect ratio $A = 5.989$

sweep back angle $\Omega = 0$

These give the following values for sternplane effectiveness and control for the current sternplanes:

sternplane $\Delta Z_w = -.03402$

$Z_{\delta_s} = -.02405$

Sternplane Cantilever Moment

For a strength assessment, it is necessary to estimate the maximum cantilever moment on the sternplane actuator shaft. This requires knowledge of the sternplane load and its center of pressure (CP). The CP is usually located between the quarter chord line and the leading edge in the chordwise direction and at, or just outboard of, a spanwise location $4/(3\pi)$ of the semi-span from the pedestal. Slender body theory puts the chordwise location of the CP of a low aspect ratio appendage at the leading edge while 2D (infinite aspect ratio) thin airfoil theory puts the CP at the quarter chord line. Recent experiments have shown that the CP can be well forward of the quarter chord line at low incidence angles but at high incidence (high load), the CP moves back to, and even aft of, the quarter chord line, especially at stall. The same experiments show the spanwise location of the CP varying from outboard of the $4/(3\pi)$ location at low incidence to slightly inboard of this location at high incidence angles.

Designing for the high load case, we assume the sternplane CP is on the quarter chord line a distance $4/(3\pi)$ of the deflectable semi-span out from the pedestal. The sternplane shaft will be axially located opposite this location to minimize actuation torque during high loads. The shaft is supported at the hull so the cantilever arm is the distance between the hull and the CP:

$$\text{cantilever arm} = \frac{4}{3\pi} \frac{b-d}{2l}$$

where the arm length has been nondimensionalized by hull length l .

For Dorado, incidence angles will always be small but sternplane control deflections will be high. And, as explained below, the loads for pitch control are about twice what they are for roll control. Therefore, the critical case for determining the maximum actuator bending moment is a pitch control deflection (synchronous sternplane deflections). The total normal force on the sternplanes and hull for this case is estimated by $Z_{\delta_s} \delta_s$. According to

Pitts *et al* [2], slender body theory predicts that the portion of this load acting on the deflecting appendages only is obtained by again multiplying by the factor $1/(1 + \lambda)$. Dividing by two to get the force on one plane and multiplying by the cantilever arm we find the critical cantilever moment Mc derivative for the current sternplane to be:

$$Mc_{\delta_s} = \frac{1}{3} \frac{|Z_{\delta_s}| (b - d)}{(1 + \lambda) \pi l}$$

$$= .0002745$$

Sternplane Roll Control

Roll control is implemented by differentially deflecting the sternplanes. When this happens, two important phenomena occur which are unique to differential deflections. First, consider the difference in the load distribution on an isolated wing when each half is deflected uniformly (pitch control) and differentially (roll control). For pitch control, the load is symmetrical about the centerline and is actually maximum at the centerline where the pressure distributions from each half reinforce each other. For roll control, the load is asymmetrical and must be zero on the centerline; the pressure distributions generating the opposing lift on each side tend to cancel each other. For a low aspect ratio wing, the net effect is that the rolling moment from one side of a differentially deflecting wing is only half that from one side of a uniformly deflecting wing (see De Young [5]).

Second, with uniform sternplane deflections, the velocity field that is generated is symmetrical about the vertical centerplane through the hull. So there is no interference with the vertical tailplane appendages. For differential sternplane deflections, however, crossflow is present at the centerplane (resulting from sternplane tip and strong hull bound vorticity) which generates a moment on the vertical appendages counteracting the moment developed by the sternplanes themselves (Adams and Dugan [6]).

So there are three good reasons why roll control is best implemented with ailerons located well outboard of the hull centerline:

- differential lift (opposing pressure distributions) is not compromised by the close proximity of the lifting components,
- crossflow on the centerplane is minimized, thereby minimizing roll reduction from interaction of the crossflow with vertically oriented appendages on the centerplane, and

- rolling moment is maximized because of the larger moment arm.

For these reasons, it makes good sense to implement roll control on the Dorado mast rather than its sternplanes. Doing so provides the added benefit of allowing the sternplanes to be devoted entirely to pitch control. However, roll control on the mast requires an additional system, one that cannot be developed in time for Build 3.

De Young [5] uses slender body theory to analyse the roll control generated by differentially deflected components on an isolated wing. If the deflecting components are symmetrical about the centerline and are the all-movable ends of the wing, and λ is the ratio of the nondeflecting inner portion of the span length to the overall span length, then the dimensionless moment generated by differentially deflecting each wing component an angle δ_o is:

$$W(\lambda, A) = 2 \frac{\frac{\partial}{\partial \delta_o} \text{moment}}{\rho U^2 S_A b}$$

$$= \frac{1}{6} (1 - \lambda^2)^{(3/2)} A$$

where $W(\lambda, A)$ is a ‘wing’ alone function and $A = b^2/S_A$ is the aspect ratio of the wing.

When the nondeflecting inner portion is replaced with a circular body with a symmetrical vertical fin (with the same planform as the sternplanes), so the differentially deflecting ends of the wing are now the sternplanes themselves, Adams and Dugan [6] use slender body theory to show that the dimensionless moment $WBF(\lambda, A)$ (for ‘wing, body, and fin’) is a complicated numerical integration of an elliptic function. Their plotted results can be fit with:

$$WBF(\lambda, A) = (.127 (1 - \lambda^2)^{(3/2)} + 2.043 \lambda^2 (1 - \lambda)^2 - 1.979 \lambda^2 (1 - \lambda)^4 - 2.543 \lambda^3 (1 - \lambda)^2 - .661 \lambda^{13} (1 - \lambda)^2) A$$

where $\lambda = d/b$.

Dorado’s vertical appendages are actually different sizes than its sternplanes (the vertical stabilizer above the hull has longer span and chord lengths and the rudder below the hull has a shorter span). However, the interaction with the vertical appendages occurs from circulation nominally in the plane of the sternplanes. This circulation interacts primarily with the root areas of the vertical fins; tip span will be less important. And from a slender body theory perspective, chord length does not effect lift. Therefore, we make the assumption that there is enough vertical fin span present above and below the hull to ensure the inertaction modelled in the $WBF(\lambda, A)$ function is effectively realized, and that any additional span or chord length discrepancies do not contribute significantly to the

interaction. That is, the $WBF(\lambda, A)$ function will be used as is.

The $WBF(\lambda, A)$ function is a pure slender body theory prediction of the moment. It needs to be modified to account for the moderate aspect ratio and the effect of the boundary layer. This is accomplished by multiplying by the ratio:

$$\frac{L_{\alpha_{estimated}}}{L_{\alpha_{slender\ body\ theory}}}$$

Using the Whicker and Fehlner formula for isolated wing lift and Dempsey's sternplane efficiency factor:

$$\frac{\partial}{\partial \alpha} L_{\alpha_{estimated}} = 1.8 \frac{\pi \eta_s(\Lambda) Q b^2}{1.8 + \cos(\Omega) \sqrt{\frac{A^2}{\cos(\Omega)^4} + 4}}$$

where Q is the dynamic pressure of the flow. In slender body theory:

$$\begin{aligned} L_{\alpha} &= (K_{W(B)} + K_{B(W)}) L_W \\ &= (1 + \lambda)^2 L_W \end{aligned}$$

and:

$$\begin{aligned} L_W &= \frac{1}{2} \pi Q (b - d)^2 \alpha \\ &= \frac{1}{2} \pi Q (1 - \lambda)^2 b^2 \alpha \end{aligned}$$

so that:

$$\frac{\partial}{\partial \alpha} L_{\alpha_{slender\ body\ theory}} = \frac{1}{2} \pi Q b^2 (1 - \lambda^2)^2$$

Thus:

$$\frac{L_{\alpha_{estimated}}}{L_{\alpha_{slender\ body\ theory}}} = 3.6 \frac{1 - .2556 \Lambda \sqrt{1 - .1612 \Lambda^2} - .6366 \arcsin(.4015 \Lambda)}{\left(1.8 + \cos(\Omega) \sqrt{\frac{A^2}{\cos(\Omega)^4} + 4} \right) (1 - \lambda^2)^2}$$

and:

$$K_{\delta_o} = \frac{WBF(\lambda, A) S_A b L_{\alpha_{estimated}}}{l^3 L_{\alpha_{slender\ body\ theory}}}$$

$$= .0009361$$

where:

$$\begin{aligned}\Lambda, \lambda &= .5480, .4146 \\ \Omega &= 0 \\ A &= 5.989 \\ b &= 2.132\end{aligned}$$

Foreplane Forces

The tools for obtaining the foreplane effectiveness, depth control derivative, and the maximum actuator cantilever moment have all been described above. We start with foreplane effectiveness.

The overall lift increment generated by attaching foreplanes to the parallel midbody section of the hull with the the vehicle at angle of attack α is:

$$\begin{aligned}L_{\alpha} &= (K_{W(B)} + K_{B(W)}) L_W \\ &= (1 + \lambda)^2 L_W\end{aligned}$$

so that:

$$\Delta Z_w = -1.8 \frac{(1 - \lambda^2)^2 \pi b^2}{\left(1.8 + \cos(\Omega) \sqrt{\frac{a^2}{\cos(\Omega)^4} + 4} \right) l^2}$$

since:

$$(1 + \lambda)^2 (b - d)^2 = (1 - \lambda^2)^2 b^2$$

The control derivative is, as before:

$$Z_{\delta_f} = \frac{\Delta Z_w}{1 + \lambda}$$

The maximum cantilever moment the foreplane actuator shaft must sustain is determined by:

$$Mc_{\delta_f} = \frac{1}{3} \frac{|Z_{\delta_f}| (1 - \lambda) b}{(1 + \lambda) \pi l}$$

The current foreplane parameters are:

$$\begin{aligned}\text{leading edge root coordinates } (x,y) &= (1.910, .5842) \\ \text{chord} &= .356 \\ \text{tip-to-tip span } b &= 2.150 \\ \lambda &= .5433\end{aligned}$$

exposed wing aspect ratio $a = 2.758$

sweep back angle $\Omega = 0$

so that:

foreplane $\Delta Z_w = -.03710$

$Z_{\delta_f} = -.02404$

$Mc_{\delta_f} = .0001979$

New Sternplane Design

The objective of the new design is to substantially increase control. This is accomplished by increasing the chord and span of the sternplane. We assume the new sternplane uses the same shaft location as the old and this determines its axial location on the hull (meters):

shaft axial location, local hull radius $= 7.159, .417$

The trailing edge will have no sweep. The leading edge will be swept back at a 20 degree angle. A sweptback leading edge is common on submarine appendages. It results in a tapered appendage with a thick base for a large, robust shaft. The taper also approximates a low drag elliptic planform and the sweptback leading edge tends to shed obstacles.

With the leading edge sweepback fixed at 20 degrees, a unique sternplane planform is specified by two parameters: root chord c_{root} (defined at the leading edge root) and either the tip-to-tip span b or the tip chord c_{tip} . In the design plots that follow, C , B , and C_{tip} are normalized versions of these parameters; they are all normalized by the values of the current design.

The loads are also normalized by those from the current design. Thus:

$$\frac{\text{New Pitch Control}}{\text{Current Pitch Control}} = \frac{Z_{\delta_s}}{[Z_{\delta_s}]_{\text{build 1}}}$$

$$\frac{\text{New Roll Control}}{\text{Current Roll Control}} = \frac{K_{\delta_o}}{[K_{\delta_o}]_{\text{build 1}}}$$

The design plot in Figure 2 shows how pitch control varies with root chord, with either the span or tip chord held constant. The second design plot (Figure 3) shows how roll control varies with the same parameters.

**Fig. 2: Pitch Control vs. Root Chord at Fixed Span (Red)
or Tip Chord (Blue) Lengths; Sweepback = 20 Degrees**

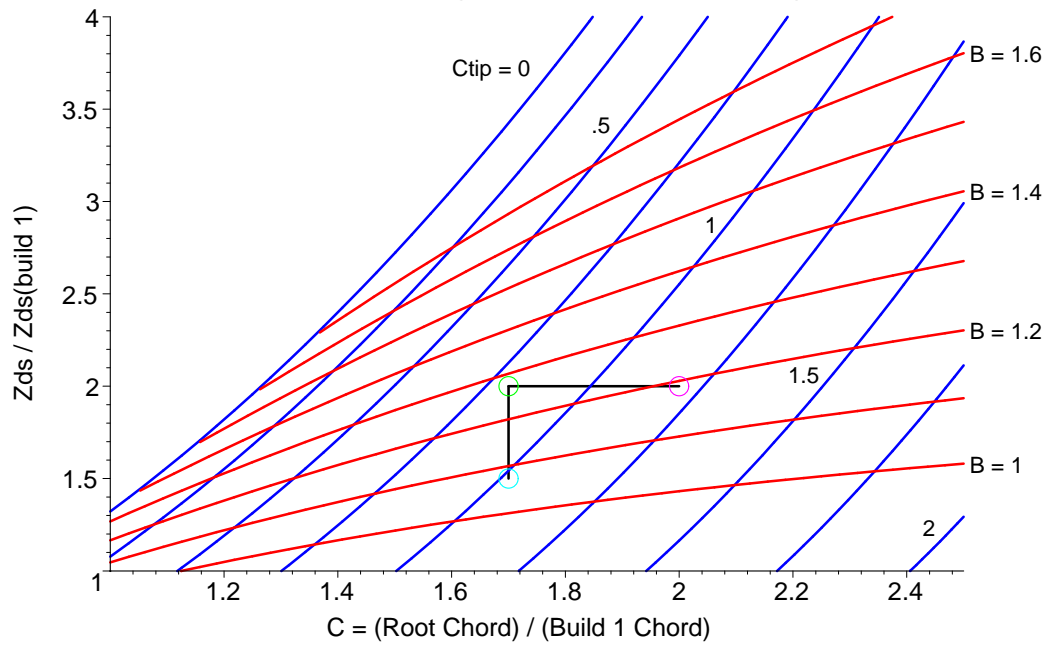
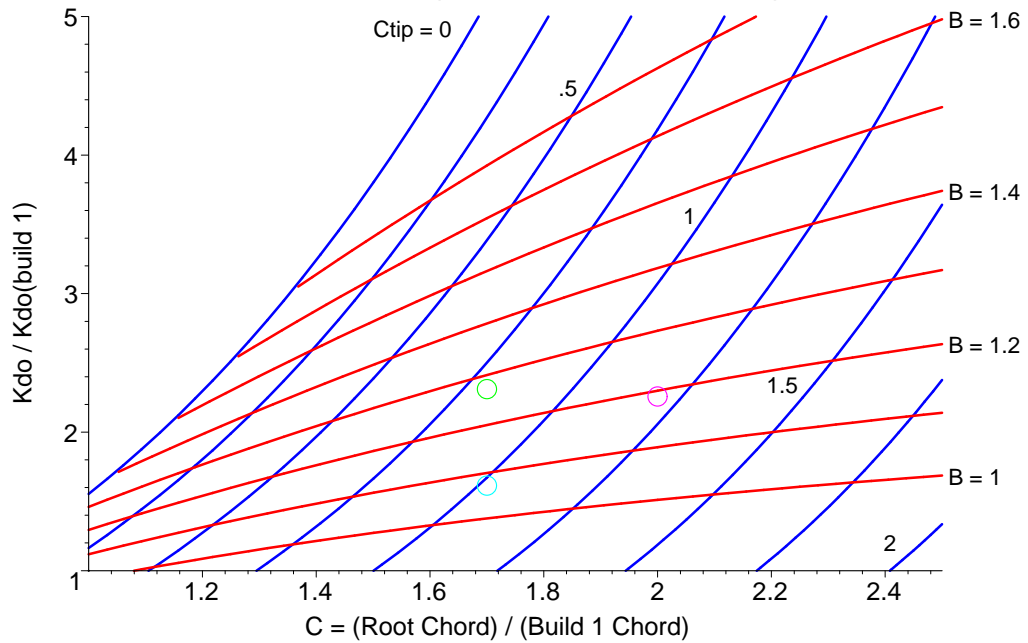


**Fig. 3: Roll Control vs. Root Chord at Fixed Span (Red)
or Tip Chord (Blue) Lengths; Sweepback = 20 Degrees**



In selecting a new design we look for two things. First, we want a thickness to chord ratio of about 15%. This should increase the maximum lift coefficient and reduce the profile drag relative to the current 25% thick sections. However, the root thickness must be maintained to accommodate the current actuator shaft diameter. Thus, the new root chord must be at least 1.67 times larger than the Build 1 chord length.

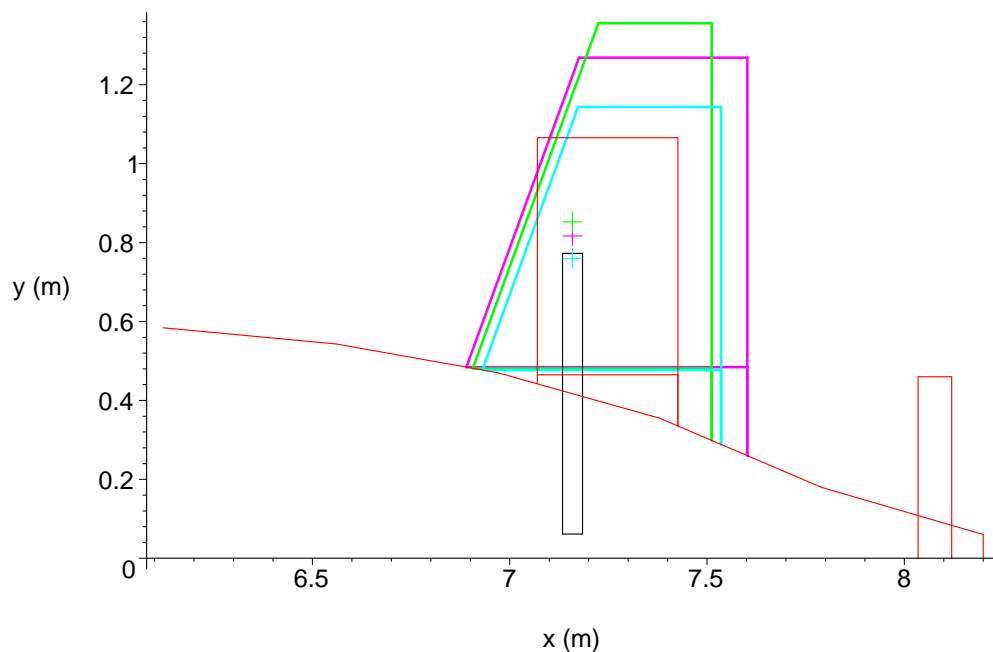
Secondly, we want control to increase between 50 and 100%.

These criteria are used for selecting three possible designs. In the design plots, these designs fall along the vertical line $C = 1.7$ for a Z_{δ_s} increase from 1.5 to 2 (slightly larger

K_{δ_o} increases), and along the horizontal line defining a Z_{δ_s} increase of 2 ($C = 1.7$ to 2).

The three designs are shown in Figure 4 superimposed over the Build 1 geometry shown in red. The colors used for the new designs in Figure 4 match those of the circles defining the design points in Figures 2 and 3.

Fig. 4: The Build 1 (thin red line) and Three Sweptback Designs and Their Design CP's (+)



Sternplane Normalized Parameters								
DESIGN	ROOT CHORD	TIP CHORD	SPAN	Delta	Z_w	Z_{δ_s}	K_{δ_o}	Mc_{δ_s}
build 1	1.00	1.00	1.00	1.00		1.00	1.00	1.00
cyan	1.70	1.02	1.07	1.50		1.50	1.61	1.60
green	1.70	.81	1.27	1.92		2.00	2.31	2.93
magenta	2.00	1.20	1.19	1.95		2.00	2.26	2.57

DESIGN	Sternplane Coordinates (m)							
	x LE ROOT	x LE TIP	x TE	y LE ROOT	y TIP	y TE ROOT	x CP	y CP
cyan	6.930	7.173	7.536	.477	1.144	.289	7.159	.760
green	6.906	7.225	7.512	.481	1.356	.299	7.159	.853
magenta	6.890	7.176	7.602	.484	1.269	.260	7.159	.817

The first table here shows how the geometry changes relative to the original design. It also shows the relative changes in:

ΔZ_w Sternplane effectiveness, the normal force derivative increment due to the presence of the sternplanes. This determines vertical plane pitch stability.

Z_{δ_s} Pitch control, the degree to which the normal force changes with sternplane deflection δ_s . This is used in Dorado to control the pitch angle of the vehicle.

K_{δ_o} Roll control, the degree to which the rolling moment changes with differential sternplane deflections.

Mc_{δ_s} Cantilever moment derivative, how the cantilever moment varies with sternplane deflection at the critical (from a stress point of view) sternplane hull junction.

Assuming twice the current control is required, the author has a preference for the magenta over the green design. The magenta design increases the span by less than 20% and has a more robust tip geometry. It provides enough chord to maintain a reasonable thickness to chord ratio while simultaneously allowing for a thickened actuator shaft at the root. The green design requires less actuator torque (see below), provides slightly better roll control because its CP is further outboard, and has a 12% lower L/b^2 ratio (downwash at the propeller) than the magenta design, but at the expense of a longer span and a higher pedestal moment (without room to thicken the actuator shaft). In short, the magenta design is the least intrusive and most robust design.

Magenta Design Characteristics

leading edge root coordinates $(x,y) = (6.890, .4842)$

$c_{root}, c_{tip}, c_A = .7120, .4265, .6574$

tip-to-tip span $b = 2.537$

$\Lambda, \lambda = .4605, .3817$

effective aspect ratio $A = 3.859$

sweep back angle $\Omega = 20$

Magenta Design Loads

The maximum torque requirement for the sternplane actuator will be 3 to 4 times that of Build 1. The load is twice as large and the average exposed chord is 1.6 times larger so the product of the two is the minimum increase in torque (the torque is proportional to the chordwise displacement of the actuator shaft from the actual CP location - an undesirable but, nevertheless, inevitable offset that is proportional to the chord length). In addition, the new design will have a higher maximum lift coefficient because (1) the 15% thickness to chord ratio optimizes this characteristic [7] and (2) its lower aspect ratio (4 versus 6) will delay the onset of stall.

The maximum required torque estimate is based on the load from one sternplane $Z_{\delta_s}/2$ reduced by $1/(1 + \lambda)$ to get the load on the sternplane alone. It is assumed that the sternplane achieves maximum lift at $\delta_s = 25$ degrees and that the chordwise offset between the CP and the actuator shaft is within 1/5 of the mean chord. Both these numbers are thought to be high and, therefore, conservative. There results:

$$\begin{aligned} \text{maximum torque} &= \frac{1}{20} \frac{|Z_{\delta_s}| \delta_s Q l^2 (c_{root} + c_{tip})}{1 + \lambda} \\ &= 790.5 \text{ } N m \\ &= 583.0 \text{ } ft lb \end{aligned}$$

where Q is the dynamic pressure at 10 knots. At 15 knots, for the same assumptions, the torque increases by a factor of $(15/10)^2 = 2.25$. The green design, which carries the same load, has a 22% shorter mean chord and so its maximum torque would be 22% smaller than the magenta design.

The actuator shaft should be able to withstand a bending moment at the sternplane root of 3 to 4 times that of Build 1. This is determined by the $M c_{\delta_s}$ normalized value in the first of the above tables. The tabulated value for the magenta design is 2.57 and the discussion in the previous paragraph regarding the higher maximum lift coefficient suggests a higher factor should be allowed for.

The maximum bending moment at the root is:

$$\begin{aligned} \text{maximum bending moment at root} &= M c_{\delta_s} \delta_s Q l^3 \\ &= 2311. \text{ } N m \\ &= 1705. \text{ } ft lb \end{aligned}$$

again for $\delta_s = 25$ degrees at a speed of 10 knots. At 15 knots, the bending moment is 2.25 times greater. It is 14% larger for the green design at any speed.

Drag has not been accounted for in these load estimates since it is expected to be smaller than the error in the estimates.

The numerical load estimates are subject to error from the linear analysis and in estimating sternplane effectiveness. This latter error is known to be as much as 50% of the load in some extreme cases so a large safety factor is recommended.

New Foreplane Design

The decision to create a new foreplane design came after the sternplane design had been fixed and its manufacture begun. The objective of a new foreplane is also to substantially increase control by increasing both its span and chord lengths. However, additional requirements were that:

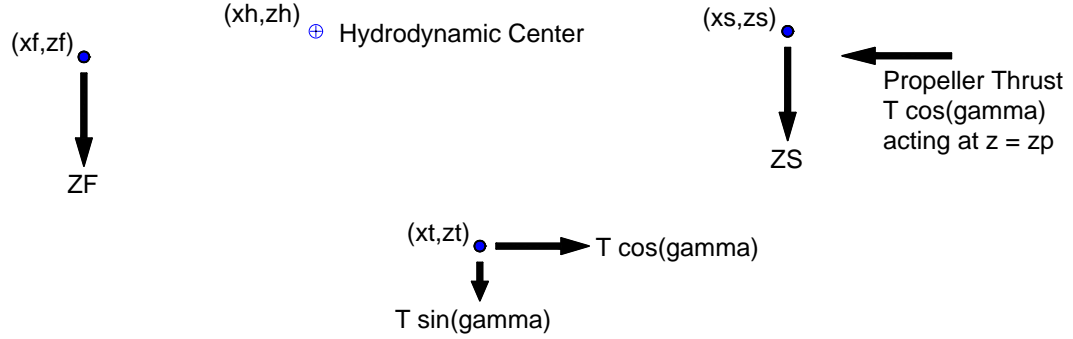
- the trailing foreplane vortex should be kept as far inboard of the sternplane tip as possible, so that extreme up and downwash velocities generated on either side of the vortex core are averaged out over the sternplane span.
- the foreplane geometry must match the end of the sternplane geometry, thereby allowing both the fore and sternplanes to be made from a single mold and ensuring that the same molded rubber bumper can be applied to the tips of both planes.

Thus, the only variable in the foreplane design is its span length. To help in deciding how large the foreplane should be, consider the following analysis of the current worst-case loads on the Dorado vehicle.

When running at close to 10 knots with the towfish at maximum depth, tow cable tension is close to 4500 pounds. The tow cable is attached at the bottom of the keel, about 1.6 m below the vehicle center line, and pulls on Dorado at an angle γ about 10 degrees below the horizontal. Although the vertical component of the force is less than 900 lbs, the horizontal component generates a large nose down pitching moment that must be overcome primarily by the sternplanes generating a downwards force well aft of the hydrodynamic center. So the nominal lift the foreplanes must generate is the vertical component of cable tension plus the downwards force generated at the sternplanes, which is by far the largest component. The analysis below shows this in more detail.

We consider a simplified view of the hydrodynamic forces. We assume the objective of the fore and sternplanes is to keep the vehicle level and that, when level, the pitching moment generated by tow cable tension and the associated propulsive force is much larger than any other moment present. Therefore, in this balance of forces, we consider only those forces from the fore and sternplanes, the tow cable, and the propeller. These forces are shown in Figure 5.

Fig. 5: Dominant Deep Tow, Even Keel Forces



The sum of these forces and the moments they generate must be zero for the vehicle to maintain the desired equilibrium:

$$ZF + ZS + T \sin(\gamma) = 0$$

$$ZF (x_f - x_h) + ZS (x_s - x_h) + T (x_t - x_h) \sin(\gamma) - T (z_t - z_h) \cos(\gamma) + T (z_p - z_h) \cos(\gamma) = 0$$

The solution of these equations is:

$$ZS = \frac{-\sin(\gamma) (x_f - x_t) T + \cos(\gamma) T (-z_t + z_p)}{x_f - x_s}$$

$$= -.5626 T \sin(\gamma) + .2703 \cos(\gamma) T$$

$$= .1685 T$$

$$ZF = \frac{\sin(\gamma) (-x_t + x_s) T + \cos(\gamma) T (z_t - z_p)}{x_f - x_s}$$

$$= -.4374 T \sin(\gamma) - .2703 \cos(\gamma) T$$

$$= -.3421 T$$

where:

$$x_f - x_h = -1.701 \text{ m}$$

$$x_s - x_h = 3.459 \text{ m}$$

$$x_t - x_h = 1.202 \text{ m}$$

$$z_t - z_h = 1.575 \text{ m}$$

$$z_p - z_h = .18 \text{ m}$$

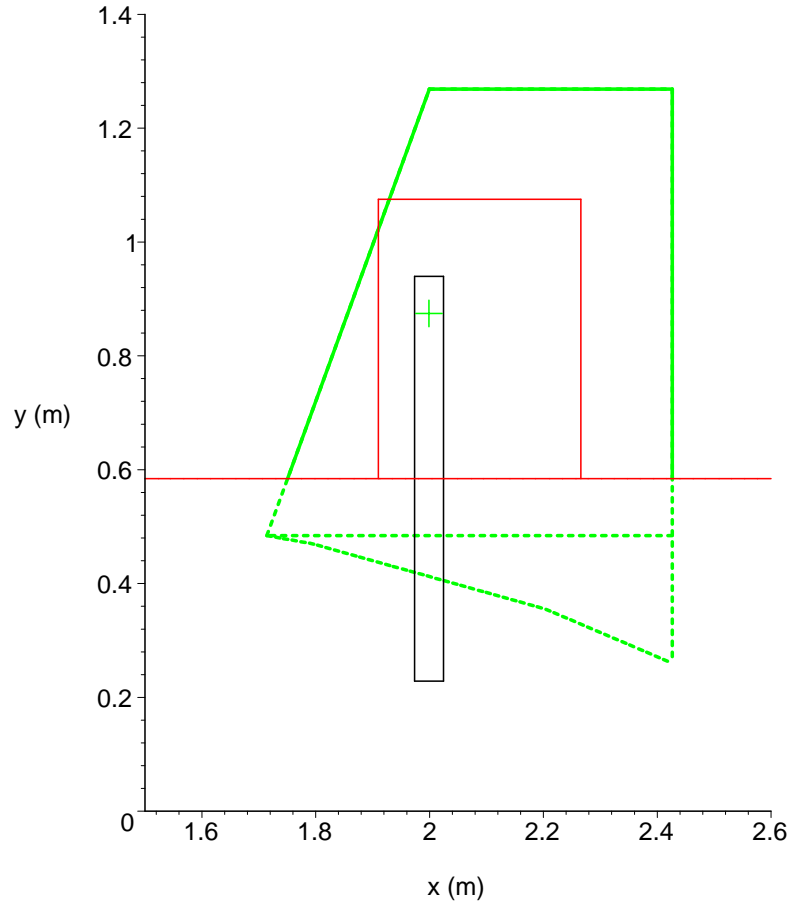
$$\gamma = \frac{1}{18} \pi$$

Thus, the horizontal tension component ($\cos(\gamma)$ term) loads the fore and sternplanes equally while the vertical tension component ($\sin(\gamma)$ term) unloads the sternplanes and loads the foreplanes. The net result is that the foreplanes must carry twice the load of the sternplanes. However, the sternplanes have two functions: pitch and roll control. Both are equally important and it is appropriate to associate half the sternplane capacity with each function. So fore and sternplane capacity is effectively balanced, then, if their normal force control derivatives are the same. The design presented below comes close to this goal.

Dorado is also fitted with fore and aft ballast tanks, although automatic ballast control has not been implemented. It is only by manually controlling these ballast tanks that the current vehicle can attain the high tow loads described above. One can envision an automated variable ballast control system, working with a response time at least an order of magnitude longer than the planes response time, that keeps the time averaged deflection of the planes close to zero. Thus, it is not necessarily a requirement that the planes be capable of supporting the full tension load by themselves. Nevertheless, as shown below, the new planes will be capable of doing so.

Figure 6 presents the foreplane design (solid green line) that balances the new sternplane pitch control capability. This design has the same span as the new sternplanes. The red lines give the current hull and foreplane geometry. The dashed green lines inside the hull give the profile of the new sternplane, for comparison purposes. Outside the hull, of course, the sternplane profile exactly matches the foreplane since they have the same span.

Fig. 6: The Build 1 (red) and New (solid green) Foreplane and its Design CP (+)



Foreplane Normalized Parameters							
DESIGN	ROOT	TIP					
	CHORD	CHORD	SPAN	Delta	Z_w	Z_delta_f	Mc_delta_f
build 1	1.00	1.00	1.00	1.00		1.00	1.00
green	1.90	1.20	1.18	1.81		1.91	2.81

Foreplane Coordinates (m)								
DESIGN	x LE	x LE	x	y LE	y	y TE	x	y
	ROOT	TIP	TE	ROOT	TIP	ROOT	CP	CP
green	1.751	2.000	2.426	.584	1.269	.584	1.999	.875

The above tables show that the green design provides 91% more depth control than the current foreplanes. Its span is the same as the sternplane span. Estimates for the fore and sternplane normal force derivatives are:

$$Z_{\delta_f}, Z_{\delta_s} = -.04586, -.04808$$

and their ratio is:

DRDC Atlantic TM 2002-048

$$\frac{Z_{\delta_f}}{Z_{\delta_s}} = .9539$$

which almost meets the fore/sternplane balancing requirement that this ratio be 1.

With a 20,000 N (4500 lb) tow cable tension at the tow point, the fore and sternplane forces required to maintain an even keel are:

$$ZF, ZS = -6843. N, 3370. N$$

Using the normal force derivatives, and assuming a 10 knot speed, the new fore and sternplane deflections required to provide these forces are:

$$\delta_f = 9.356 \text{ degrees}$$

$$\delta_s = -4.395 \text{ degrees}$$

which is satisfactory. These are steady state forces and the planes need to reserve a good amount of capacity to handle unsteady forces that will be superimposed on them. In addition, of course, the sternplanes must accomodate roll control requirements, a function they are not well suited for and which may, therefore, require a disproportionate amount of the sternplane capacity.

Note that the foreplane wake impinging on the sternplanes will be primarily downwash. And downwash will generate some of the desired nose-up pitching moment on the sternplanes even when they are not deflected. This effect has not been factored into the estimates, but it is a beneficial one. As previously mentioned, the concern with downwash is the high velocities in the core of the trailing vortex and the unsteady forces they can generate when the vortex position changes as the vehicle maneuvers.

Green Design Characteristics

leading edge root coordinates $(x,y) = (1.751, .5842)$

root, tip chord lengths = .6756, .4265

tip-to-tip span $b = 2.537$

$\lambda = .4605$

exposed wing aspect ratio $a = 2.484$

effective aspect ratio $A = 3.859$

sweep back angle $\Omega = 20$

Green Design Loads

The maximum torque requirement for the foreplane actuator will be about 3 to 4 times that of Build 1. This is because the load and mean chord are 91 and 55% greater, respectively,

than the Build 1 design. And the new design will likely have a higher maximum lift coefficient.

The maximum required torque estimate is based on the load from one foreplane $Z_{\delta_f}/2$ reduced by $1/(1 + \lambda)$ to get the load on the foreplane alone. It is, again, conservatively assumed that the foreplane achieves maximum lift at $\delta_s = 25$ degrees and that the chordwise offset between the CP and the actuator shaft is $1/5$ of the mean chord. This gives:

$$\begin{aligned} \text{maximum torque} &= \frac{1}{20} \frac{Z_{\delta_f} \delta_f Q l^2 (c_{root} + c_{tip})}{1 + \lambda} \\ &= 690.6 \text{ } N \text{ } m \\ &= 509.4 \text{ } ft \text{ } lb \end{aligned}$$

where Q is the dynamic pressure at 10 knots.

The actuator shaft should be able to withstand a bending moment at the foreplane root between 3 and 4 times that of Build 1. This is determined by the normalized Mc_{δ_f} value in the first of the above tables. This value is 2.81 and since higher lift coefficients are expected, a higher factor should be allowed for.

The maximum bending moment at the root is estimated as:

$$\begin{aligned} \text{maximum bending moment at root} &= Mc_{\delta_f} \delta_f Q l^3 \\ &= 1820. \text{ } N \text{ } m \\ &= 1342. \text{ } ft \text{ } lb \end{aligned}$$

again for $\delta_f = 25$ degrees at a speed of 10 knots.

Minimizing Actuator Torque Requirements

The above maximum torque estimates may require the use of larger fore and sternplane actuators than are currently in place. However, full scale experimentation can minimize this requirement. Consider the following procedure.

At low incidence angles, appendage load is smallest and the CP is furthest forward. As incidence increases, the CP moves aft.

- Build and install the planes as designed, using readily available actuators.

- Instrument the shafts or actuators so that shaft torque and appendage load can be measured.
- Run the vehicle at speed and deflect the planes through their full range of angles while measuring the loads. If the actuators cannot generate enough torque to fully deflect the planes, reduce speed (ie, Q) until full deflection is achieved.

These measurements provide the chordwise location of the CP as a function of load. The chordwise location of the shaft can then be changed so that the maximum torque is minimized. And, of course, the maximum torque will also be known. This could substantially reduce the maximum torque requirement quoted above.

If load measurements are not available, it may still be possible to carry out some variation of this procedure based only on torque measurements. However, this would require more trial and error.

Appendage Drag During Deep Tow Conditions

The drag from the new planes, when generating the same control loads as the current planes do at their limits, will likely be lower than the drag on the current planes. This is mainly because the new design has increased effectiveness and will not be operating at its limits where stall and trailing edge separation greatly increase drag. However, since the new design is capable of generating higher lift, it is also capable of generating higher drag (induced drag increases with the square of the lift).

When the new planes are being used to keep an even keel while towing at depth, without aid from the ballast tanks, fore and sternplane lifts of 6800 N and -3400 N, respectively, are required. The induced drag associated with this lift is estimated using a formula for an isolated wing from Whicker and Fehlner [3]:

$$C_D = C_{d_0} + \frac{C_L^2}{\pi A e}$$

where the dimensionless C coefficients are based on planform area S . C_{d_0} is the minimum section drag coefficient, C_L is the lift coefficient and $e = 0.9$ is the Oswald efficiency factor. The incremental drag associated with deflecting the planes is therefore:

$$\Delta D = 2 \frac{L^2}{\rho U^2 \pi b^2 e}$$

Using the ZF, ZS worst case tow cable tensions at 10 knots (given above) we have:

$$\Delta D_f = 189.3 \text{ N}$$

$$\Delta D_s = 45.92 \text{ N}$$

$$\Delta D_f + \Delta D_s = 235.2 \text{ N}$$

This amounts to just over 1% of the horizontal component of tension on the vehicle. So the additional drag from equilibrium being maintained by control surfaces rather than ballast is not a major concern from a system efficiency point of view.

Adding the magnitudes of the induced drag components here is a conservative approach. Overall induced vehicle drag is probably more correctly estimated by using the net lift (3400 N) in the induced drag formula. This would lead to a much smaller induced drag estimate. In any case, the parasitic drag on the vehicle, $C_{d_0} = 3500 \text{ N}$, together with the tow cable tension, 20,000 N, is much larger than the induced drag from the plane loads.

Discussion

The new fore and sternplane designs are shown in more detail in the Appendix.

The empirical tools used in this report are based on experiments with appendages similar to those proposed here. The thickness to chord ratios of these appendages are typically 15% and are constant along the tapering span (so the thickness tapers too). This is also the practice followed with submarine appendages and is recommended for the new designs.

Whicker and Fehlner [3] suggest the crossflow drag coefficient for a wing is about twice as large for unfaired as for faired wing tips. This means the wing generates more lift at high incidences (second order lift - not accounted for in the above analysis) with unfaired tips. No doubt drag and flow noise also increase with an unfaired tip, even at low incidence angles. It is probably best to fair the tips to reduce in-transit drag. The current practice of using rounded rubber bumpers on the plane tips seems like a good one.

All wings develop lift by sustaining a pressure difference between their upper and lower surfaces. This pressure difference is maximum at the center span location and gradually diminishes towards the tips, providing a spanwise loading distribution that closely resembles an ellipse. Gaps in a wing at inboard spanwise locations, such as must exist between the inboard end of the deflecting sternplane and its pedestal, or the foreplane and the hull, equalize the pressure across the wing reducing its lift. This effect is not accounted for in the estimates in this report, but can be significant [8]. The manufacturing process should try to minimize these gaps by building accurate pedestals for the sternplanes and, perhaps, shoring up the hull opposite the foreplanes.

End plates are currently used on Dorado control surfaces at the plane tips and at the inboard end of the deflecting portion of the plane. End plates are thought to increase lift at the cost of a drag penalty, but their performance is not well understood. It is unusual to find the simple form seen on Dorado on modern submarines and aircraft, although a more refined version (winglets - a bit delicate for Dorado's environment) is becoming prevalent. The author's preference is to not use end plates with the new planes unless a deficiency is identified which they might address.

It is expected that the maximum lift coefficients on the new planes will occur for δ values around 20 degrees. The lift will probably decrease past stall but the drag will increase sharply. It would be worthwhile to strain gauge the actuator shafts of the new sternplanes in order to identify the maximum lift angle, and then limit deflection accordingly. This might be done in parallel with the actuator torque minimization procedure discussed above.

Concluding Remarks

Design plots are presented for redesigning the Dorado Build 1 sternplanes. From these, three improved designs are examined and one is selected. The proposed new sternplanes have a 20% longer span and, on average, a 60% longer chord. This provides twice the control of the Build 1 design. The design uses the same actuator shaft location as Build 1.

A new foreplane design is chosen which balances the new sternplane capabilities for the worst-case, deep tow condition. The new foreplane has a 18% longer span and 55% longer chord, providing 91% more depth control than the current foreplanes using the same actuator shaft. Its span matches the sternplane span. This design comes from the end of the new sternplane design, so they can be built from the same mold.

The new designs require actuators that generate from 3 to 4 times more torque than is required of the current ones. The actuator shafts should be redesigned to support as much as four times the current bending moment at the sternplane root.

The new designs use a tapered appendage together with increased chord to reduce the thickness to chord ratio from 25 to 15%. This should delay the onset of stall and reduce drag for a given load.

The new planes should be able to handle worst-case tow loads with moderate steady state deflections, leaving an appreciable portion of their capacity for dealing with unsteady loads.

References

- [1] J.R. Spreiter and A.H. Sacks, “The Rolling Up of the Trailing Vortex Sheet and Its Effect on the Downwash Behind Wings,” *Journal of the Aeronautical Sciences*, vol. 18, no. 1, January 1951.
- [2] W.C. Pitts, J.N. Nielsen, G.E. Kaattari, “Lift and Center of Pressure of Wing-Body-Tail Combinations at Subsonic, Transonic, and Supersonic Speeds,” NACA Report 1307, 1957.
- [3] L.F. Whicker and L.F. Fehlner, “Free-Stream Characteristics of a Family of Low-Aspect-Ratio, All-Movable Control Surfaces for Application to Ship Design,” DTMB Report 933, December 1958.
- [4] E.M. Dempsey, “Static Stability Characteristics of a Systematic Series of Stern Control Surfaces on a Body of Revolution,” DTNSRDC Report 77-0085, August 1977.
- [5] J. De Young, *Spanwise Loading For Wings and Control Surfaces of Low Aspect Ratio*, NACA Technical Note 2011, January 1950.
- [6] G.J. Adams and D.W. Dugan, *Theoretical Damping in Roll and Rolling Moment Due to Differential Wing Incidence for Slender Cruciform Wings and Wing-Body Combinations*, NACA Report 1088, 1952.
- [7] I.H. Abbott and A.E. von Doenhoff, “Theory of Wing Sections,” Dover, 1959.
- [8] D.W. Dugan, “Experimental Investigation of Some Aerodynamic Effects of a Gap Between Wing and Body of a Moderately Slender Wing-Body Combination at a Mach Number of 1.4,” NACA RM A55D08, May 1955.

APPENDIX A: Sternplane Magenta Design

The section profile for the Magenta design is a NACA 0015 thickness distribution. This profile is given by Abbott and von Doenhoff [7]:

$$\eta(\xi) = .2226750000 \sqrt{\xi} - .09450000000 \xi - .2637000000 \xi^2 + .2132250000 \xi^3 - .07612500000 \xi^4$$

for:

$$0 \leq \xi \leq 1.$$

Here, η is the half thickness of the profile, ξ is the chordwise coordinate, and the origin is at the leading edge. Both η and ξ are normalized by the local chord length. The leading edge thickness is zero but the trailing edge thickness is nonzero, about 0.3% of the chord length. This is the profile for a 15% thick section, so $2\eta_{max} = 0.15$.

Because of the 20 degree leading edge sweepback, the leading edge x coordinate for the spanwise profile is:

$$x_{le}(y) = .3639702342 y$$

where x and y are in meters with their origins at the leading edge root.

The spanwise chord length variation is:

$$c(y) = .7120000000 - .3639702342 y$$

Combining the above three equations gives the equation for the top half of the sternplane surface:

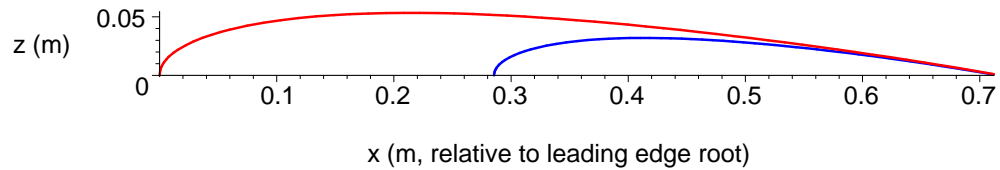
$$z(x, y) = c(y) \eta\left(\frac{x - x_{le}(y)}{c(y)}\right)$$

The RHS of $z(x, y)$ is written out in ASCII format for copying into other programs.

```
(.2226750000*((x-.3639702342*y)/(.7120000000-.3639702342*y))^(1/2)-.9450000000e-1*(x-.3639702342*y)/(.7120000000-.3639702342*y)-.2637000000*(x-.3639702342*y)^2/(.7120000000-.3639702342*y)^2+.2132250000*(x-.3639702342*y)^3/(.7120000000-.3639702342*y)^3-.0761250000e-1*(x-.3639702342*y)^4/(.7120000000-.3639702342*y)^4)*(.7120000000-.3639702342*y)
```

Setting $y = 0$ (the leading edge root spanwise location) and $y = 0.7843$ (the tip) in $z(x, y)$, the following 2D half-profiles can be drawn:

Fig. 7: The L.E. Root (red) and Tip (blue) Section Profiles



The sternplane pedestal is mounted on the hull. The hull profile is not well known but it defines the inner surface of the pedestal. The pedestal outer surface must be flat and perpendicular to the rotation axis (parallel to the hull centerline) so the deflecting sternplane does not bind. This outer surface is located 1/2 inch = 0.0127 m outboard of the root leading edge spanwise location. The current actuator shaft has a diameter of 2 inches and extends 14 inches out from the hull. The gap between the outer pedestal surface and the inner surface of the deflecting sternplane should be minimized.

Two figures are shown below. Figure 8 is a 3D rendering of the sternplane and actuator shaft and Figure 9 is a line drawing of the planform.

Fig. 8: Magenta Design - Starboard Sternplane

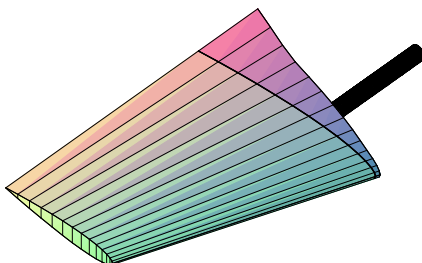
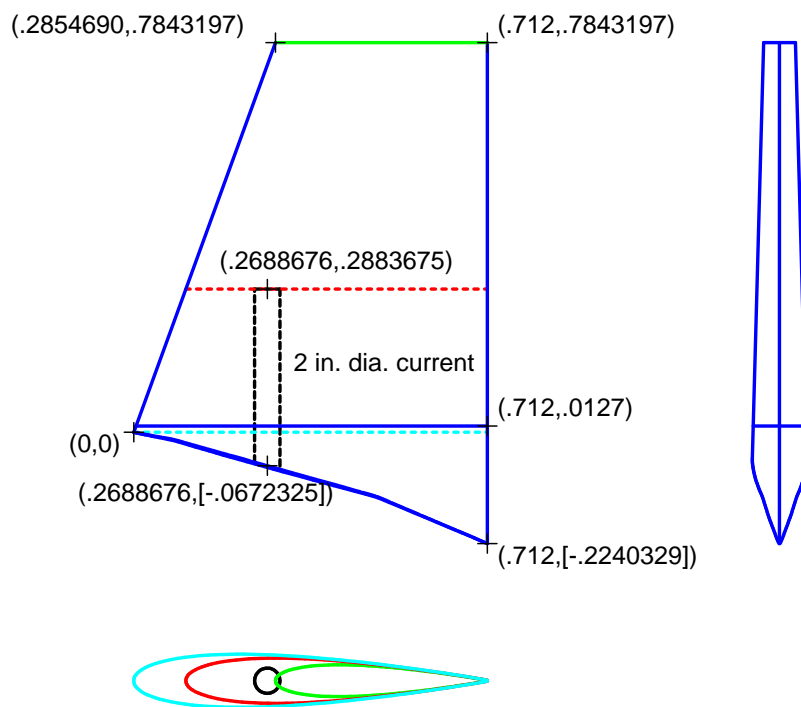


Fig. 10: Magenta Design - Line Drawing

Dimensions in meters. [] surround nominally correct values.



APPENDIX B: Foreplane Green Design

The green design uses the same planform and section profiles as the magenta design. The tips match exactly but the foreplane root leading edge is about 10 cm out from the sternplane root leading edge. The green design leading edge is therefore also given by:

$$x_{le}(y) = .3639702341 y$$

where x and y are in meters with their origins at the leading edge root. However, the spanwise chord length variation is different:

$$c(y) = .6756103761 - .3639702342 y$$

The equation for the top half of the foreplane surface is again:

$$z(x, y) = c(y) \eta \left(\frac{x - x_{le}(y)}{c(y)} \right)$$

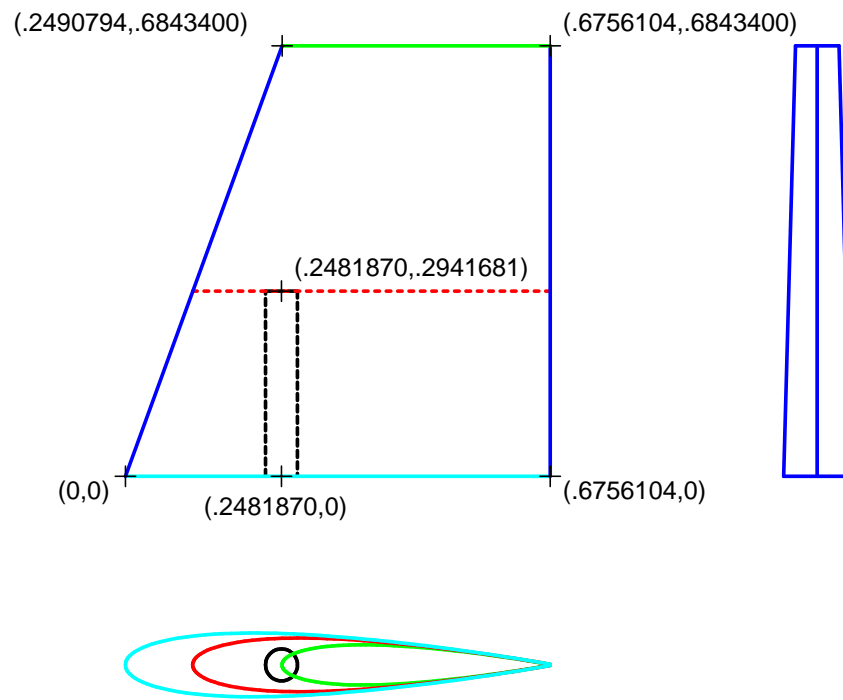
and the ASCII version of the RHS of $z(x, y)$ is:

```
(.2226750000*((x-.3639702341*y)/(.6756103761-.3639702342*y))^(1/2)-.94500
00000e-1*(x-.3639702341*y)/(.6756103761-.3639702342*y)-.2637000000*(x-.36
39702341*y)^2/((.6756103761-.3639702342*y)^2+.2132250000*(x-.3639702341*y)
^3/((.6756103761-.3639702342*y)^3-.7612500000e-1*(x-.3639702341*y)^4/((.675
6103761-.3639702342*y)^4)*(.6756103761-.3639702342*y)
```

The foreplane planform is shown in the linedrawing of Figure 10.

Fig. 11: Green Design - Line Drawing

Dimensions in meters.



APPENDIX C: Mold Geometry

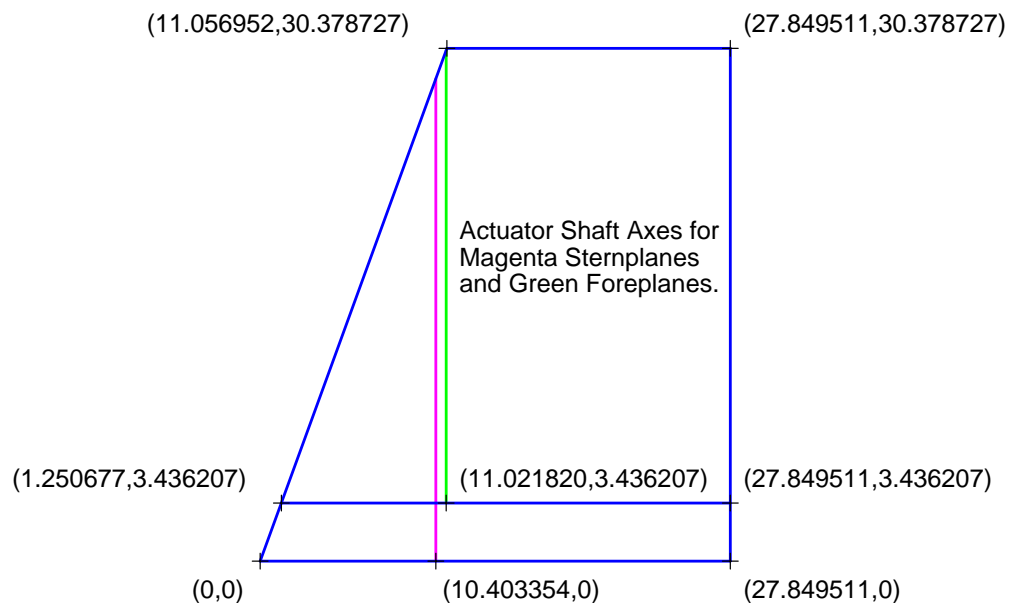
A female mold will be machined for laying up fiberglass planes. The mold will be in two halves, joined by bolts and dowels. Each half of the mold will be in two pieces, also joined by bolts and dowels. With the pieces joined together, the mold is for a sternplane. With the smaller bottom piece removed, the mold is for the foreplane. The planform for one-half of the mold is shown below; the other half of the mold is a mirror image of this half.

The mold span is 0.0127 m (1/2 inch) short of the sternplane span shown in Appendix A to accommodate the pedestal. The origin in the mold planform drawing is shifted to the root leading edge of the mold. In the coordinate system shown in Appendix A, this new origin is located at:

$$x, y = .004622421974 \text{ m}, .01270000000 \text{ m}$$

In addition, the dimensions have been converted to inches for this drawing as the draftsman and machine shop use this system of units.

**Fig. 12: Dorado Fore and Sternplane Mold Planform
(x,y) coordinates in inches**



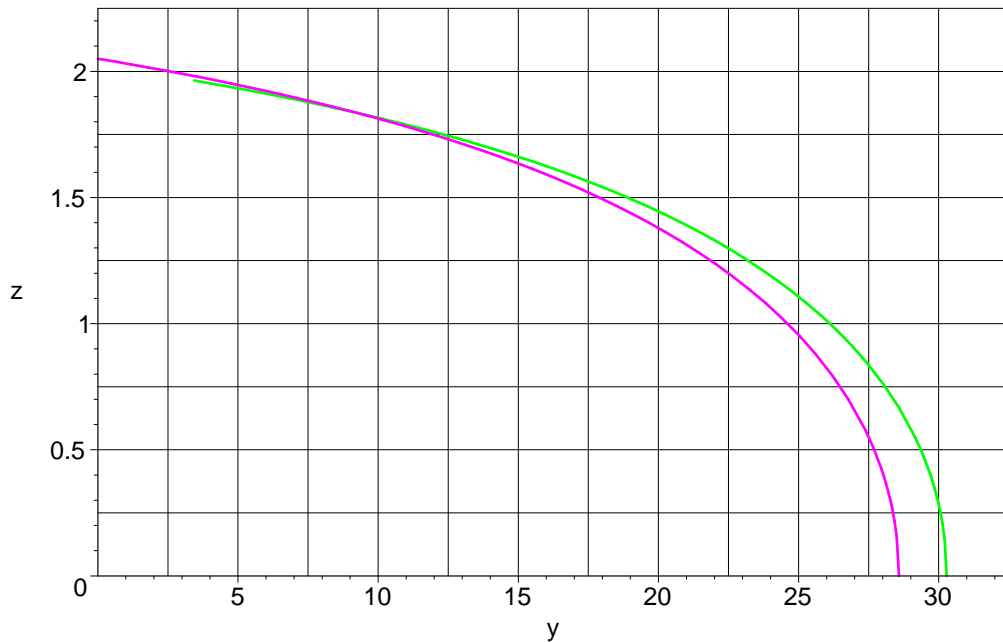
This drawing also shows the locations of the actuator axes relative to the mold coordinate system. The shafts are inserted in the mold during manufacture. Thus the thickness

distribution along the axes is needed for deciding what shaft size can be accommodated. This distribution is found from the equation for the wing surface in mold coordinates (inches):

$$39.37007874 * (.2226750000 * ((.2540000000e-1 * x - .9244843949e-2 * y) / (.7073775780 - .9244843949e-2 * y))^{(1/2)} - .9450000000e-1 * (.2540000000e-1 * x - .9244843949e-2 * y) / (.7073775780 - .9244843949e-2 * y) - .2637000000 * (.2540000000e-1 * x - .9244843949e-2 * y)^2 / (.7073775780 - .9244843949e-2 * y)^2 + .2132250000 * (.2540000000e-1 * x - .9244843949e-2 * y)^3 / (.7073775780 - .9244843949e-2 * y)^3 - .7612500000e-1 * (.2540000000e-1 * x - .9244843949e-2 * y)^4 / (.7073775780 - .9244843949e-2 * y)^4) * (.7073775780 - .9244843949e-2 * y)$$

The figure below shows the thickness distributions (the *outer* surface of each plane) along the axes. These are obtained by setting x to the appropriate constant in the above equation for the surface.

**Fig. 12: Mold Half-Thickness Distribution (inches)
Along Actuator Shaft Axes**



Machining Considerations

The mold will be cut using a ball nosed cutter. The radius of the cutter is determined by the minimum radius in the mold. Aside from the sharp trailing edge corner, which requires a special cutter, the minimum radius occurs at the nose of the tip profile. It is [7]:

$$\begin{aligned} \text{tip section nose radius} &= 1.1019 \frac{t^2}{c} \\ &= .4163337048 \text{ in} \end{aligned}$$

where $t/c = 0.15$ is the section thickness to chord ratio and:

$$c = 16.79255850 \text{ in}$$

is the tip chord length. Thus, a 1 inch diameter cutter, having a radius of 1/2 inch, is too large but a 3/4 inch diameter cutter is fine.

The trailing edge is a problem area for mold manufacture. The trailing edge half-thickness $t/2$ is obtained in mold coordinates by setting x to the trailing edge x coordinate:

$$x_{te} = 27.84951094 \text{ in}$$

in the above equation for the mold surface, giving (in inches):

$$\frac{1}{2} t_{te} = .04386297972 - .0005732531189 y$$

So the trailing edge half thicknesses at the sternplane mold root and tip are:

$$\frac{1}{2} t_{te, root} = .043862986 \text{ in}$$

$$\frac{1}{2} t_{te, tip} = .02644828048 \text{ in}$$

The slope of the section profile at the trailing edge is obtained by differentiating the above expression for the surface and setting $x = x_{te}$. The arctan of this slope gives the angle of the profile line relative to the chord line.

$$\text{profile slope at trailing edge} = -.1753875000$$

$$\text{profile slope as an angle} = -9.947786463 \text{ degrees}$$

The slope is independent of the spanwise coordinate y because the sections are geometrically similar; that is, the ratio of a y dimension to an x dimension (and slope = rise/run) does not change as the size of the profile changes.

The trailing edge region of the mold needs to be machined with a cutter specially ground to fit the trailing edge corner and profile slope. It helps that the slope is the same all along the span right at the trailing edge. However, the profile changes in the chordwise direction faster over the radius of the cutter for the tip profile than for the root profile. If we give the cutter an angle that matches the slope of the tip profile 3/8 inch forward of the trailing edge:

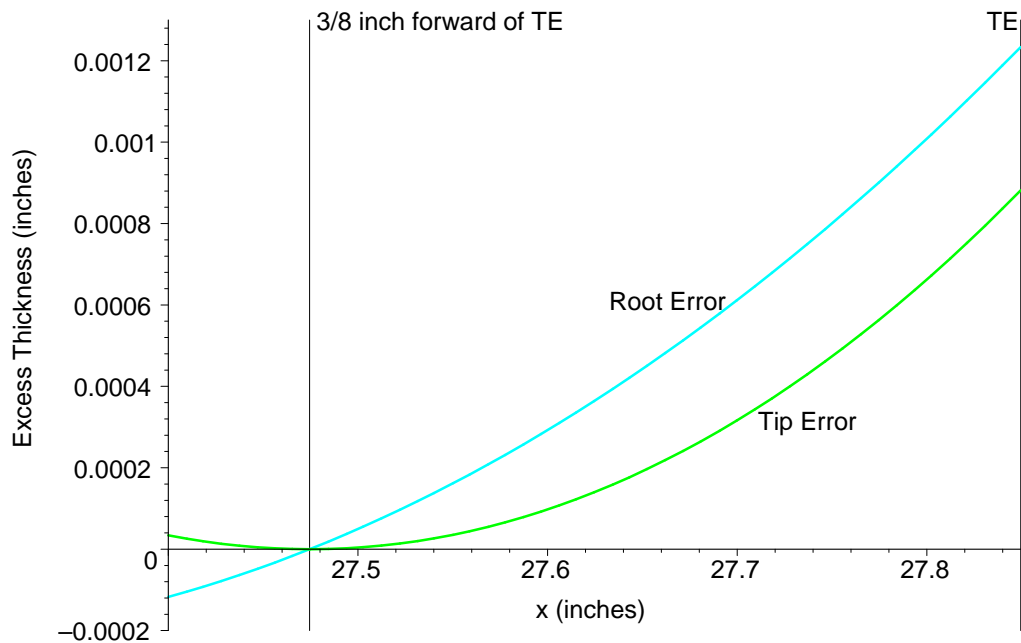
$$\text{tip profile angle } 3/8 \text{ inch from TE} = -9.684163234 \text{ degrees}$$

then the cutter will leave too thick a trailing edge when it matches the profile from the ball cutter 3/8 inch from the trailing edge. In addition, there will be a slight discontinuity in the

slope at the 3/8 inch location for other than the tip profile. However, this discontinuity is largest at the root where it is off by only :

.103254548 *degrees*

The excess trailing edge thickness that results from this approximation is of the order of one thousandth of an inch, as shown in the sketch below. These errors are acceptable at the trailing edge.



To facilitate release of the fiberglass from the mold at the trailing edge, it will be necessary to round over the trailing edge corner. This can be done by putting a radius on the trailing edge cutter. A corner radius of 0.025 inches will round over almost all the tip trailing edge and most of the root trailing edge.

DOCUMENT CONTROL DATA		
(Security classification of title, body of abstract and indexing annotation must be entered when the overall document is classified)		
1. ORIGINATOR (the name and address of the organization preparing the document. Organizations for whom the document was prepared, e.g. Establishment sponsoring a contractor's report, or tasking agency, are entered in section 8.)	2. SECURITY CLASSIFICATION (overall security classification of the document including special warning terms if applicable).	
Defence Research and Development Canada - Atlantic	UNCLASSIFIED	
3. TITLE (the complete document title as indicated on the title page. Its classification should be indicated by the appropriate abbreviation (S,C,R or U) in parentheses after the title).		
Dorado Build 1 Fore and Sternplane Redesign		
4. AUTHORS (Last name, first name, middle initial. If military, show rank, e.g. Doe, Maj. John E.)		
Watt, George D.		
5. DATE OF PUBLICATION (month and year of publication of document)	6a. NO. OF PAGES (total containing information Include Annexes, Appendices, etc).	6b. NO. OF REFS (total cited in document)
September 2002	45	8
7. DESCRIPTIVE NOTES (the category of the document, e.g. technical report, technical note or memorandum. If appropriate, enter the type of report, e.g. interim, progress, summary, annual or final. Give the inclusive dates when a specific reporting period is covered).		
DRDC Atlantic Technical Memorandum		
8. SPONSORING ACTIVITY (the name of the department project office or laboratory sponsoring the research and development. Include address).		
Defence Research and Development Canada – Atlantic, P.O. Box 1012, Dartmouth, Nova Scotia, Canada, B2Y 3Z7		
9a. PROJECT OR GRANT NO. (if appropriate, the applicable research and development project or grant number under which the document was written. Please specify whether project or grant).	9b. CONTRACT NO. (if appropriate, the applicable number under which the document was written).	
11GL-12		
10a. ORIGINATOR'S DOCUMENT NUMBER (the official document number by which the document is identified by the originating activity. This number must be unique to this document.)	10b. OTHER DOCUMENT NOS. (Any other numbers which may be assigned this document either by the originator or by the sponsor.)	
DRDC Atlantic TM 2002-048		
11. DOCUMENT AVAILABILITY (any limitations on further dissemination of the document, other than those imposed by security classification)		
<input checked="" type="checkbox"/> Unlimited distribution <input type="checkbox"/> Defence departments and defence contractors; further distribution only as approved <input type="checkbox"/> Defence departments and Canadian defence contractors; further distribution only as approved <input type="checkbox"/> Government departments and agencies; further distribution only as approved <input type="checkbox"/> Defence departments; further distribution only as approved <input type="checkbox"/> Other (please specify):		
12. DOCUMENT ANNOUNCEMENT (any limitation to the bibliographic announcement of this document. This will normally correspond to the Document Availability (11). However, where further distribution (beyond the audience specified in (11) is possible, a wider announcement audience may be selected).		

13. **ABSTRACT** (a brief and factual summary of the document. It may also appear elsewhere in the body of the document itself. It is highly desirable that the abstract of classified documents be unclassified. Each paragraph of the abstract shall begin with an indication of the security classification of the information in the paragraph (unless the document itself is unclassified) represented as (S), (C), (R), or (U). It is not necessary to include here abstracts in both official languages unless the text is bilingual).

The Dorado semi-submersible remote minehunting vehicle requires increased pitch, roll, and depth control while towing its sonar at depth. The vehicle controls both pitch and roll using independently deflectable sternplanes. Depth is controlled with foreplanes. New fore and sternplane designs are proposed which double control authority with about a 20% increase in span length and a 60% increase in average chord length. The new designs require from 3 to 4 times more actuator torque to achieve control and the actuator shaft bending moment will be up to 4 times larger. However, the new plane designs should allow the vehicle to maintain depth and equilibrium with only moderate control deflections while towing the sonar at depth.

14. **KEYWORDS, DESCRIPTORS or IDENTIFIERS** (technically meaningful terms or short phrases that characterize a document and could be helpful in cataloguing the document. They should be selected so that no security classification is required. Identifiers, such as equipment model designation, trade name, military project code name, geographic location may also be included. If possible keywords should be selected from a published thesaurus. e.g. Thesaurus of Engineering and Scientific Terms (TEST) and that thesaurus-identified. If it not possible to select indexing terms which are Unclassified, the classification of each should be indicated as with the title).

submarines
underwater vehicles
hydrodynamics
sternplanes
foreplanes
bowplanes

This page intentionally left blank.

Defence R&D Canada

**Canada's leader in defence
and national security R&D**

R & D pour la défense Canada

**Chef de file au Canada en R & D
pour la défense et la sécurité nationale**



www.drdc-rddc.gc.ca